Journal of the American Association for Laboratory Animal Science
Copyright 2025
by the American Association for Laboratory Animal Science

Vol 64, No 3
May 2025
Pages 364–373

Minimal Xenograft Tumor Growth Variability in Nude Mice Infected with *Corynebacterium bovis* as a Single Pathogenic Agent

Alanna G Backx, DVM, MSc, DACLAM,[1,†] Hilda R Holcombe, DVM, PhD, DACLAM,[1] Magalie Boucher, DVM, MS, DACVP,[1] Anthony Mannion, PhD,[1] Theresa M Albers, DVM, DACVP,[2] Kenneth S Henderson, PhD, MS,[2] Guy B Mulder, DVM, MS, MBA, DACLAM,[2] and Aurora A Burds, PhD[3,*]

Reduced xenograft engraftment and delayed tumor growth in immunocompromised mice have been associated with infection by *Corynebacterium bovis*, a highly contagious bacterium that causes sporadic clinical disease and chronic shedding. To learn what effect *C. bovis* infection may have on the reproducibility of preclinical cancer studies, subcutaneous tumors were monitored in male and female nude (*Foxn1*^{nu}) mice topically infected with *C. bovis* 2 to 3 weeks prior to cell injection (chronically infected) or at the time of cell injection (acutely infected) and compared with tumors in uninfected control mice. There were largely no significant differences in tumor engraftment rates, final tumor weights, or final tumor volumes between infection groups for any of the 3 established human cell lines; that is, SJSA-1, an osteosarcoma; HT-29, a colorectal adenocarcinoma; and A549, a lung carcinoma. However, HT-29–engrafted tumors grew significantly more slowly in acutely infected males than in the chronically infected or uninfected males, although no difference was present between the HT-29–engrafted female groups. No epidermal hyperplasia or hyperkeratosis was present in either of the infected groups, compared with the controls, which paralleled the absence of scaly skin clinically across all groups. In summary, our results suggest that *C. bovis* as a single pathogenic agent may have a limited effect on xenograft engraftment and growth. Investigators using different strains of immunocompromised mice, different cell lines, or mice housed in facilities with different health status from that described in the present study but endemic for *C. bovis* should perform pilot studies to determine whether tumor engraftment and/or growth is affected by infection.

Abbreviations and Acronyms: AC, acutely infected; CAH, *Corynebacterium*-associated hyperkeratosis; CHR, chronically infected; CNT, uninfected control; NS, not significant; qPCR, quantitative PCR

DOI: 10.30802/AALAS-JAALAS-24-137

Introduction

Corynebacterium bovis is a highly contagious bacterium that can cause sporadic clinical disease and chronic shedding in immunocompromised mice.[1–4] Although not observed in all mice, the most defining clinical manifestation is *Corynebacterium*-associated hyperkeratosis (CAH), or 'scaly skin disease,' in nude (*Foxn1*^{nu}) mice. The presence of *Staphylococcus xylosus*, an opportunistic pathogen in immunocompromised mice,[5,6] can complicate *C. bovis* surveillance since this bacterium can also cause alopecia in haired mice and crusts and scaly skin in nude and haired mice, closely resembling CAH. *Staphylococcus xylosus* is not excluded from most SPF barriers, and it is possible that coinfection with *C. bovis* causes or exacerbates the clinical dermatitis associated with these 2 organisms.[5,6] In addition, *S. xylosus* typically outgrows *C. bovis* in culture, complicating the detection of *C. bovis* if bacterial culture is the only diagnostic screening test used.

In facilities with endemic *C. bovis* infection, chronic carriers shed bacteria in aerosols, which contaminate the environment and spread infection between cages.[7] Contaminated tumor tissue will also act as a source of transmission of the pathogen if transplanted.[8] The organism can be detected by PCR or culture,[1,8] but a survey conducted in 2017 found that testing was not routinely performed in many National Cancer Institute–designated Comprehensive Cancer Centers.[9] Eradication is costly and difficult when infection is widespread, requiring complete depopulation/repopulation or rederivation and thorough environmental and equipment decontamination.[2,7,10] Moreover, reinfection of shared facilities can occur within months and can preclude any attempts at eradication. Maintenance of a *C. bovis*–free health status in immunocompromised mice requires diligent testing and uniform compliance from all investigators; this is especially difficult in large academic facilities with shared equipment and high turnover of investigators and trainees.

Adding to the difficulty in staff and investigator commitment to the stringent requirements for long-term eradication is the absence of controlled, peer-reviewed studies on the negative impacts of *C. bovis* infection on tumor engraftment or growth in immunocompromised mice. To date, only postoutbreak comparisons have been made, and these studies failed to examine the potential role of coinfection with *S. xylosus* or other organisms.[4,9,11,12] In addition, *C. bovis*–positive mice were found

Submitted: 18 Nov 2024. Revision requested: 17 Dec 2024. Accepted: 13 Mar 2025.
[1]Division of Comparative Medicine, Massachusetts Institute of Technology, Cambridge, Massachusetts; [2]Research Models and Services, Charles River Laboratories, Wilmington, Massachusetts; and [3]Koch Institute for Integrative Cancer Research, Massachusetts Institute of Technology, Cambridge, Massachusetts
**Corresponding author. Email: aaburds@mit.edu*
[†]Current affiliation: Animal Care Services, Queen's University, Kingston, Ontario, Canada.
This article contains supplemental materials online.

Downloaded from https://prime-pdf-watermark.prime-prod.pubfactory.com/ at 2025-08-31 via free access

to have higher-than-expected mortality following administration of a chemotherapeutic agent,[13] decreased engraftment of 2 human solid tumor cell lines in nude but not NSG mice,[11] and variable transplant success of primary patient-derived xenograft leukemia in NSGS mice that express human IL-3, GM-CSF, and stem cell factor.[9,12] The findings in NSGS mice were subsequently published in a peer-reviewed journal, making it the first publication to demonstrate a negative impact of *C. bovis* on (solid or blood) tumor engraftment in an immunocompromised mouse model.[4] However, no study has correlated the timing of *C. bovis* infection xenograft growth rates and success in nude mice.

This study was designed to determine whether *C. bovis* infection as a single pathogenic agent alters the growth parameters of xenografted tumors in nude mice. We also investigated whether the timing of infection relative to the date of cell injection varied the effect on tumor growth. We hypothesized that the level of tumor growth inhibition in *C. bovis*–infected mice depends on both the phenotype of the cell line and the timing of infection, with acutely infected (AC) individuals showing an increase in tumor growth inhibition. We also hypothesized that mice infected with *C. bovis* prior to tumor induction (chronic carrier state) would demonstrate less growth inhibition and variability as compared with mice acutely infected at the time of injection, but that both groups would have some tumor rejection.

Materials and Methods

Animals and husbandry. Male and female, 4- to 5-wk-old, outbred nude (Crl:NU-*Foxn1*^{nu}) mice were supplied by Charles River Laboratories (Wilmington, MA). This stock was chosen because it is the stock from which the *C. bovis* isolate used in this study was originally collected (see below). Mice were naive to any experimental manipulations and were confirmed to be negative for murine viruses (Murine respirovirus (formerly Sendai virus), pneumonia virus of mice, *Betacoronavirus muris* (previously described as mouse hepatitis virus), Protoparvovirus rodent1 (includes strains previously described as mouse parvovirus and minute virus of mice), *Cardiovirus theileri* (previously described as Theiler's murine encephalomyelitis virus), reovirus, mouse rotavirus, mouse adenovirus, polyomavirus, K virus, murine cytomegalovirus, mouse thymic virus, lymphocytic choriomeningitis virus, Hantaan virus, ectromelia virus, lactate dehydrogenase–elevating virus, genogroup V norovirus, and murine chapparvovirus), pathogenic bacteria (*Bordetella bronchiseptica*, *Filobacterium rodentium*, *C. bovis*, *Corynebacterium kutscheri*, *Citrobacter rodentium*, *Helicobacter* spp., *Klebsiella oxytoca*, *Klebsiella pneumoniae*, *Mycoplasma pulmonis*, *Pasteurella multocida*, *Rodentibacter heylii*, *Rodentibacter pneumotropicus*, *Proteus mirabilis*, *Pseudomonas aeruginosa*, *Salmonella* spp., *Staphylococcus aureus*, *Streptobacillus moniliformis*, *Streptococcus pneumoniae*, beta hemolytic *Streptococcus* spp., *Clostridium piliforme*), *S. xylosus*, *Pneumocystis*, and endoparasites and ectoparasites including *Encephalitozoon cuniculi* and enteric protozoa prior to shipment to MIT. Mice were housed in fully AAALAC-accredited facilities and used in accordance with protocols approved by MIT's IACUC. Standard autoclaved static microisolation cages were used and mice were provided with ad libitum access to irradiated food and autoclaved water. Cage density was set and maintained at 5 mice per cage. All holding and procedure rooms were kept at 21 to 22 °C, 30% to 70% relative humidity, and on a 12-h light/12-h dark cycle (lights on at 0700). Mice were only handled within a dedicated NuAire class II A/B3 biologic safety cabinet (all uninfected mice, including experimental infection groups prior to inoculation) or an AniGARD e3 class 10 cage transfer station (Baker, Sanford, ME) within a dedicated cubicle (experimental infection groups postinoculation). Holding rooms, procedure rooms, biologic safety cabinets, and cage transfer stations were confirmed to be negative for *C. bovis* via environmental swab and molecular testing prior to use; areas swabbed included benches, shelving, and the edge of any wall vent casings, in addition to the interior seams and air grates of the cabinets. A new, disposable coverall suit was used before handling the infected mice. Double-gloving and cage decontamination with accelerated hydrogen peroxide for at least 1 min prior to handling were used for all cages.[7] Uninfected mice and postinoculation *C. bovis*–infected mice were housed in different facilities to prevent contamination of the uninfected control (CNT) mice.[7] Each holding room had dedicated scales for weighing mice and calipers for sizing tumors. All equipment that contacted mice or their caging underwent vaporized hydrogen peroxide, ethylene oxide, or autoclave sterilization prior to use. All manipulations, husbandry, and handling, including unpacking the shipment upon arrival and biweekly cage changes, were performed by the authors.

Experimental infection. The *C. bovis* isolate used for this study (1810230001 SH1) was previously banked from an outbred nude (Crl:NU-*Foxn1*^{nu}) mouse originating at Charles River Laboratories presenting with CAH at MIT; this mouse was coinfected with *S. xylosus*. Frozen 181023001 SH1 stock was streaked on blood agar plates and incubated at 37 °C without CO_2 supplementation for 72 h. Single colonies were picked and transferred to 15 mL of brain heart infusion media with 1% Tween 80 in 50-mL conical tubes.[14] The tubes were shaken overnight at 32 °C and 250 rpm.[15] After ~19 h, when the bacteria were in the log growth phase,[14] cultures were diluted for topical inoculation. Cultures were kept at room temperature throughout dosing.

Cages of mice were assigned randomly to 1 of 3 treatment groups for each tumor type. Chronically infected (CHR) mice were inoculated with *C. bovis* 14 to 21 d prior to injection of tumor cells, at ~5 to 6 wk of age. AC mice were inoculated with bacteria at the time of tumor injection at 8 wk of age. The AC group represented exposure associated with the onset of experimental manipulation. CNT mice received a sham infection at 5 to 6 wk of age 14 to 21 d prior to injection. Each group consisted of 5 male and 5 female mice, with one cage of each sex (Figure 1). Prior to inoculation, all mice received gentle exfoliation of the dorsal cervical and intrascapular skin using 10 swipes from caudal to cranial with dry sterile gauze with the goal of creating microabrasions under isoflurane. A minimum of 7.5×10^5 cfu (range 0.75 to 6.85×10^6 cfu) of *C. bovis* in 50 µL of medium was then applied with a micropipettor. The applied dose was distributed on the exfoliated areas and around the pinna, eyes, and mouth with a sterile cotton-tipped applicator presoaked with the inoculum. A new pipette tip, aliquot, and cotton-tipped applicator were used for each cage. The final dose was confirmed with serial dilutions of an unused aliquot plated in duplicate on blood agar plates ~1 to 2 h following the inoculation procedure. CNT mice underwent a sham procedure, with the same steps, except with 50 µL of sterile medium. This dose range and application method were internally validated during a pilot study, which resulted in 100% colonization in individually housed mice (data not shown). The exfoliation step was included because it has been previously determined that intimate contact with the skin is important.[1,2]

In addition to regular clinical assessments for morbidity associated with tumor growth, as outlined below, all mice were assessed at least 4 times a week by research staff for signs of CAH and/or dermatitis, including scaling, erythema, hunching, dehydration, and weight loss.

Downloaded from Comparative Medicine Section via free access

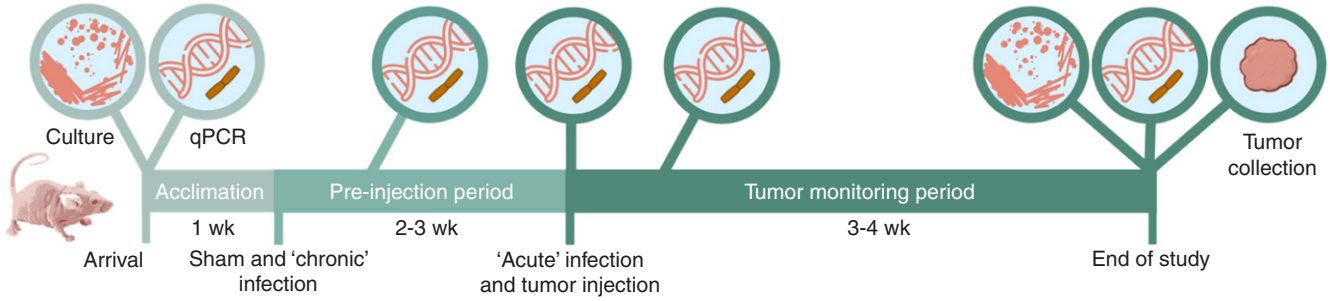

Figure 1. Experimental design. Upon arrival, 4- to 5-wk-old mice were tested by aerobic dermal culture and fecal qPCR. For each cell line, 3 groups consisting of 5 males and 5 females were created (n = 30 total): 1) chronic infection; 2) acute infection (infection groups had a minimum of 7.5×10^5 cfu applied topically); and 3) sham infection control (media only) following the timeline depicted. All 3 treatment groups were injected with tumor cells on the same day at 8 wk of age with aliquots of tumor cells expanded at the same time. Fecal qPCR testing occurred 7 d after inoculations, on the day of injection, and at the end of the study with a second dermal culture. Upon completion of each experiment, 3 to 4 wk after injection, tumors were collected and weighed, and an intrascapular skin sample was collected and formalin-fixed. Skin samples were examined microscopically and scored.

Microbial testing. All mice were tested for *C. bovis* using quantitative PCR (qPCR) from fresh fecal pellets upon arrival, at the time of tumor cell injection, 7 d after inoculation/sham inoculation, and at the end of the experiment; all mice or cages of mice were tested by qPCR at least 4 times. For all AC and CHR mice, individual animals were tested at the 7 d postinoculation mark to confirm uniform colonization, and otherwise all samples were pooled by cage. Fecal samples from CNT mice housed together were pooled. Fecal pellets were chosen since they were previously shown to be more sensitive than skin swabs, with ~10-fold more template detected on average,[16] which mirrored our findings (data not shown). Pooled swabs from cages of mice were submitted for aerobic culture to verify *C. bovis* and *S. xylosus* infection status prior to and at the end of each experiment. Culture samples were collected by rubbing a sterile, dry cotton-tipped applicator over the dorsum and around the face and neck of each mouse. Samples were cultured on blood agar/McConkey split agar, chocolate agar, and phenylethyl alcohol blood agar plates at 37 °C for 14 d. Blood agar plates were also incubated at 25 °C for 14 d. Tumor cell lines were confirmed to be negative for *C. bovis* using qPCR prior to expansion in vitro and injection.

Whole-genome sequencing and analysis. Whole-genome sequencing on genomic DNA by Illumina MiSeq was performed at the MIT BioMicro Center to confirm that the inoculum *C. bovis* strain 1810230001 SH1 (inoculum strain) and the strain recovered from our study mice, *C. bovis* strain 2305220054 (output strain), were the same. Genome sequences were assembled and annotated using the comprehensive genome analysis tool hosted by the Bacterial and Viral Bioinformatics Resource Center.[17] Sequencing data also evaluated the similarity of these strains with previously described *C. bovis* strains isolated from humans and from animals that presented with clinical disease. Average nucleotide identity analysis comparison was performed to determine the similarity between *C. bovis* genomes.[18] To further evaluate the similarity of the inoculum and cultured *C. bovis* strains, a whole-genome phylogenetic tree was built from core protein-coding genes, which provides higher resolution of strain-level phylogeny.[19]

Tumor cell lines. Three established human cancer cell lines were used: SJSA-1 (osteosarcoma), HT-29 (colorectal adenocarcinoma), and A549 (lung carcinoma). The cells were expanded in vitro according to American Type Culture Collection instructions, and cultures in the exponential growth phase were suspended in PBS for subcutaneous injection. All 3 infection groups were injected with cells on the same day at 8 wk of age. Each mouse received 100 µL with 1 to 5×10^6 cells each over the right flank as previously described.[20,21] Mouse weight and tumor size were measured 1 to 3 times weekly, as determined by the phase of growth, and experiments continued until the largest tumors for each cell type reached 15 mm in length. Tumor volume was calculated as (length × width^2)/2. All mice were monitored at least 4 times a week by research staff for overall body condition, severe clinical disease (for example, ulcerations, deep excoriations), ulcerated tumors, signs of dehydration, and anemia; these signs along with 20% weight loss were grounds for euthanasia. All mice survived to the experimental endpoint as outlined. For each tumor type, all cohorts of mice were euthanized on the same day. Upon euthanasia, PCR and culture samples were collected, tumors were removed and weighed, and skin samples were collected. All tumor and skin samples were fixed in 10% buffered formalin and embedded in paraffin for further analyses. Research staff were assigned to either the CNT or the AC and CHR groups, and tumor growth parameters were not shared between personnel until the end of each experiment as a bias-reducing measure.

Histologic analysis. For each tumor cell type, all 10 CNT mice (5 males and 5 females) and 3 males and 3 females of each of the CHR and AC groups were analyzed. Square samples of skin/subcutis (~1 × 1 cm) collected from intrascapular region were fixed in 10% formalin, processed, and then sectioned so that 2 longitudinal sections were paraffin embedded and stained with hematoxylin and eosin for histopathologic evaluation and with Gram stain to investigate bacterial presence. Hematoxylin and eosin sections were analyzed for evidence of hyperkeratosis, acanthosis, and dermatitis (inflammatory infiltrate) using standardized grading schemes on a scale of 1 to 3, as previously described.[1] Intercorneal Gram-positive–stained rod-shaped bacteria were assessed using a Gram stain of sequential section, and superficial dermal bacterial colonization was confirmed with qPCR and culture as described above.

Statistical analysis. A minimum group size of n = 4 was estimated using the NC3Rs Experimental Design Assistant power analysis with a significance level of 0.05 and power of 0.90 based on prestudy data collected at MIT in the SJSA-1 cell line with an effect size (±SD) of 300 (±100) mm^3 tumor volume.[22] Descriptive statistics were tabulated for continuous variables (body weight, tumor volume, tumor weight) and categorical variables (histologic skin inflammation score, histologic tumor assessment). The mean ± SEM tumor volume at each timepoint was determined and displayed as a growth curve and compared using a two-way ANOVA (time x treatment). For significant deviations in growth, tumor growth inhibition was calculated using the following formula at specified timepoints: 100% × (mean volume of CNT mice – mean volume of infected

Comparative Medicine Section

Downloaded from https://prime-pdf-watermark.prime-prod.pubfactory.com/ at 2025-08-31 via free access

mice)/mean volume of CNT mice. Final tumor weights were compared using an ANOVA. Histologic scores were compared using Kruskal–Wallace tests. $P \leq 0.05$ was considered statistically significant. Statistical analyses were performed using GraphPad Prism 10.0.2 (GraphPad Software, Boston, MA).

Results

Experimental infection. All mice gained weight throughout the study period, and there was no observed CAH or other types of dermatitis. Signs of impending ulceration (for example, thinning of dermis, immobility of the underlying tumor independently from skin) coincided with the 15 mm maximum tumor length across all groups within a tumor cohort, and all mice were euthanized prior to any skin or tumor ulceration. *Staphylococcus xylosus* was not isolated through aerobic dermal culture upon arrival to MIT or at the experimental endpoints; all cohorts of mice were confirmed to be *S. xylosus*–free. *Enterococcus* spp. were isolated upon arrival and at the experimental endpoints for all groups. All experimentally infected animals (CHR and AC) were positive for *C. bovis* by day 7 after experimental inoculation (individual animal tests) and remained positive throughout the study (pooled by cage tests), as demonstrated by fecal qPCR. At necropsy, *C. bovis* was cultured from the skin of infected mice injected with SJSA-1 and A549 tumor cell lines, but not the HT-29 cell line. Because the fecal pellets of the HT-29 experimentally infected cohorts repeatedly tested positive by qPCR, we suspect that the large number of *Enterococcus* spp. isolated hindered *C. bovis* growth in culture, as previously described.[2] All CNT cohorts remained negative for *C. bovis* throughout the study, as demonstrated by negative fecal qPCR and culture.

Whole-genome sequencing analysis of *C. bovis* isolates. Genome size, GC content, protein coding, and RNA genes were comparable across all available *C. bovis* genomes, including the strains isolated in this study (Table S1). Average nucleotide identity analysis comparison was performed to determine the similarity between *C. bovis* genomes. This analysis showed both *C. bovis* strains 1810230001 SH1 (inoculum strain) and 2305220054 (output strain) exhibited >99.99% similarity in average nucleotide identity, indicating conserved genetic relationships; this is expected if there was no contamination with a second strain after experimental infection. In addition, these strains demonstrated average nucleotide identity similarity >95% with other known *C. bovis* genomes (Figure 2A), confirming their taxonomic classification. *Corynebacterium bovis* strains isolated from rodents (for example, mouse and rat) with skin disease form a distinct phylogenetic clade, which included *C. bovis* strain 1810230001 SH1 and *C. bovis* strain 2305220054 (Figure 2B). *Corynebacterium bovis* strains 1810230001 SH1 and strain 2305220054 are located on the same branch within the rodent clade, indicating they are more similar to each other than other rodent genomes. *Corynebacterium bovis* strains 1810230001 SH1 and 2305220054 were also localized with another *C. bovis* strain, 1807030003 SH2, isolated from an immunocompromised mouse at MIT presenting dermatitis, suggesting strain-specific genetic divergence based on institution or geographical location. Taken together, these findings indicate that *C. bovis* strain 1810230001 SH1 (inoculum strain) and *C. bovis* strain 2305220054 (output strain) are likely identical strains and are genetically associated with other *C. bovis* strains isolated from mice with clinical CAH.

Tumor growth inhibition. The growth rates of the SJSA-1 tumors did not differ between the 3 treatment groups for both the male and females (two-way ANOVA, time x treatment, male $F_{14,84} = 1.174$, female $F_{14,84} = 0.061$, P = not significant [NS]; Figure 3A). In addition, the final recorded tumor weights were not significantly different ($F_{2,12} = 2.077$ [male], $F_{2,12} = 0.642$ [female], P = NS; Figure 3B).

The growth rate of the HT-29 tumors in the AC males was reduced compared with the CHR and CNT males ($F_{10,60} = 3.635$, $P = 0.0008$; Figure 3A). The inhibited growth was apparent in the AC males, compared with the CNT males, by 17 d postinjection (Tukey's honestly significant difference test, $P < 0.005$), and between the AC males and both the CHR and CNT male groups by 21 d postinjection, coinciding with the last day of the experimental period (Tukey's honestly significant difference test, $P < 0.0001$). The corresponding growth inhibition of the HT-29 tumor cell line in the AC males was 64.4% and 62.8% at 17 and 21 d postinjection, respectively, compared with the CNT males. Although the final average weights of the CNT and CHR tumors were 430.2 and 406.6 g, respectively, compared with an average of 208.3 g for the AC group, there was no significant difference between these 3 groups when comparing final tumor weights ($F_{2,12} = 1.802$, P = NS; Figure 3B). The AC male tumors showed more variability in weight than did the CNT and CHR male groups (CV 85.7% compared with 56% [CNT] and 45.2% [CHR]). The HT-29–engrafted female mice showed no significant differences between the 3 groups for both the tumor growth curves ($F_{10,60} = 1.773$, P = NS) or final tumor weights ($F_{2,12} = 0.833$, P = NS).

The final tumor type, A549, demonstrated no difference in growth rates (male $F_{10,60} = 0.662$, female $F_{10,60} = 0.773$, P = NS; Figure 3A) or final tumor weights (male $F_{2,12} = 0.279$, female $F_{2,12} = 0.495$, P = NS; Figure 3B) between the different infectious groups. The absence of negative impact on tumor growth parameters was consistent for both males and females.

Histologic analysis. Hematoxylin and eosin section analysis of skin from the CNT groups across all 3 tumor types and both sexes showed many background lesions that were considered expected, normal findings in nude mice. These findings included disintegration of the inner root sheath or the hair, resulting in twisting, coiling, and fracture of the hair shafts (Figure 4A and B), epithelial hyperplasia of follicular infundibulum and dilation by keratinaceous debris (follicular keratosis; Figure 4C), and normal hair follicle numbers, normal anagen hair bulbs, and normal sebaceous glands.[23] The CNT animals also displayed folliculitis/perifolliculitis, primarily characterized by neutrophil and/or macrophage infiltration with occasional plasma cells and rare mast cells, with or without necrotic debris (Figure 4C); this was considered to be secondary to phenotypic hair shaft dysplasia. Dermal fibroplasia was also noted, characterized by more fibroblasts and secondary formation and development of fibrous tissue (Figure 4B). Finally, the CNT groups generally had mixed populations of bacteria present, primarily within the follicular infundibulum.

The changes seen within the CHR and AC infection groups were not distinguishable from those found in the CNT groups, and there were no differences in bacterial load seen between the 3 study/tumor cohorts (Table 1). The observed bacteria in the skin sections of all groups were generally found within the infundibulum rather than within the free keratin layers separate from the hair shafts (Figure 4D), which is unlike what has been described for *C. bovis*. As such, *C. bovis* could not be conclusively visualized, even in animals with confirmed *C. bovis* infection by both PCR and aerobic dermal culture collected on the same day as the skin samples for analysis.

Discussion

To maintain the integrity of xenograft models in cancer research at our institution, and to reduce interstudy variability

Downloaded from https://prime-pdf-watermark.prime-prod.pubfactory.com/ at 2025-08-21 via free access

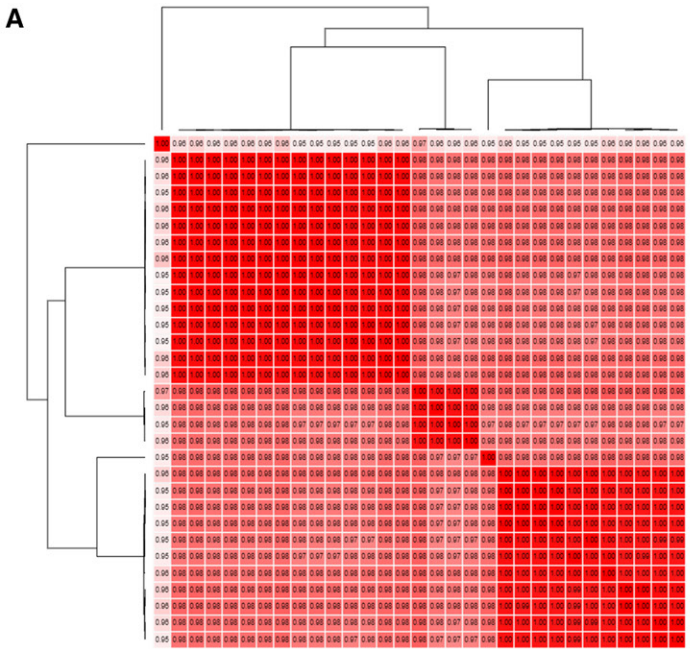

Strain	Host	Tissue or disease
Corynebacterium bovis 24956	Mouse	Skin
Corynebacterium 1810230001 SH1 (input strain)	Mouse	Dermatitis
Corynebacterium 1807030003 SH2	Mouse	Dermatitis
Corynebacterium bovis 2305220054 (output strain	Mouse	Clinically normal
Corynebacterium bovis strain 16-1683 - large	Mouse	Hyperkeratosis/acanthosis
Corynebacterium bovis strain 16-1683 - small	Mouse	Hyperkeratosis/acanthosis
Corynebacterium bovis strain 17-0240 - large	Mouse	Hyperkeratosis/acanthosis
Corynebacterium bovis strain 7894	Mouse	Hyperkeratosis/acanthosis
Corynebacterium bovis strain 16-2004	Rat	Dermatitis/ulcerative lesions
Corynebacterium bovis strain 16-3465	Mouse	Hyperkeratosis/acanthosis
Corynebacterium bovis strain 17-0240 - small	Mouse	Hyperkeratosis/acanthosis
Corynebacterium bovis strain 12-5346	Mouse	Hyperkeratosis/acanthosis
Corynebacterium bovis strain 13-1426	Mouse	Hyperkeratosis/acanthosis
Corynebacterium bovis strain CUAMC1 - large	Mouse	Hyperkeratosis/acanthosis
Corynebacterium bovis strain CUAMC1 - small	Mouse	Hyperkeratosis/acanthosis
Corynebacterium bovis ERR1332588	N/A	N/A
Corynebacterium bovis P12_C2	Human	Skin
Corynebacterium bovis strain F6900	Human	Eyes
Corynebacterium bovis strain WCM1	Human	Neck mass
Corynebacterium bovis MSK180	Human	Nasopharyngeal
Corynebacterium bovis DSM 20582	N/A	N/A
Corynebacterium bovis DSM 20582 = CIP 54.80	Cow	N/A
Corynebacterium bovis DSM 20582 = CIP 54.80	N/A	Milk
Corynebacterium bovis strain FDAARGOS_1052	N/A	N/A
Corynebacterium bovis strain 4828	Cow	Mastitis
Corynebacterium bovis strain 4826	Cow	Mastitis
Corynebacterium bovis strain MI 82-1021	Cow	Milk
Corynebacterium bovis strain WCM3 - large	Human	N/A
Corynebacterium bovis strain WCM3 - small	Human	N/A
Corynebacterium bovis strain WCM4	Human	Wound
Corynebacterium bovis strain WCM5	Human	Eye

Strain	Host	Tissue or disease	Geographic location
Corynebacterium bovis strain 4826	Cow	Mastitis	U.S.: Hawaii
Corynebacterium bovis strain MI 82-1021	Cow	Milk	U.S.: Tennessee
Corynebacterium bovis strain WCM4	Human	Wound	U.S.: New York City
Corynebacterium bovis strain WCM5	Human	Eye	U.S.: New York City
Corynebacterium bovis strain WCM3 - small	Human	N/A	U.S.: New York City
Corynebacterium bovis strain WCM3 - large	Human	N/A	U.S.: New York City
Corynebacterium bovis strain 4828	Cow	Mastitis	U.S.: Hawaii
Corynebacterium bovis DSM 20582 = CIP 54.80	N/A	N/A	U.S.: Washington, DC
Corynebacterium bovis DSM 20582	N/A	N/A	N/A
Corynebacterium bovis DSM 20582 = CIP 54.80	Cow	Milk	N/A
Corynebacterium bovis strain FDAARGOS_1052	N/A	N/A	Germany: Braunschweig
Corynebacterium bovis MSK180	Human	Nasopharyngeal	Botswana: Gaborone
Corynebacterium bovis strain WCM1	Human	Neck mass	U.S.: New York City
Corynebacterium bovis strain F6900	Human	Eyes	U.S.: Washington
Corynebacterium bovis P12_C2	Human	Skin	Denmark: Aarhus
Corynebacterium bovis ERR1332588G	N/A	N/A	U.S.
Corynebacterium bovis 24956	Mouse	Skin	U.S.: Maine
Corynebacterium bovis strain 12-5346	Mouse	Hyperkeratosis/acanthosis	U.S.: New York City
Corynebacterium bovis strain 13-1426	Mouse	Hyperkeratosis/acanthosis	U.S.: New York City
Corynebacterium bovis strain 7894	Mouse	Hyperkeratosis/acanthosis	U.S.: New York City
Corynebacterium bovis strain CUAMC1 - large	Mouse	Hyperkeratosis/acanthosis	U.S.: Colorado
Corynebacterium bovis strain CUAMC1 - small	Mouse	Hyperkeratosis/acanthosis	U.S.: Colorado
Corynebacterium bovis 2305220054 (output strain)	Mouse	Clinically normal	U.S.: MIT, Cambridge, MA
Corynebacterium 1810230001 SH1 (inoculum strain)	Mouse	Dermatitis	U.S.: MIT, Cambridge, MA
Corynebacterium 1807030003 SH2	Mouse	Dermatitis	U.S.: MIT, Cambridge, MA
Corynebacterium bovis strain 16-2004	Rat	Dermatitis/ulcerative lesions	U.S.: New York City
Corynebacterium bovis strain 16-3465	Mouse	Hyperkeratosis/acanthosis	U.S.: New York City
Corynebacterium bovis strain 17-0240 - small	Mouse	Hyperkeratosis/acanthosis	U.S.: New York City
Corynebacterium bovis strain 17-0240 - large	Mouse	Hyperkeratosis/acanthosis	U.S.: New York City
Corynebacterium bovis strain 16-1683 - small	Mouse	Hyperkeratosis/acanthosis	U.S.: New York City
Corynebacterium bovis strain 16-1683 - large	Mouse	Hyperkeratosis/acanthosis	U.S.: New York City

Figure 2. Whole-genome sequencing of *Corynebacterium bovis* strains. Fields where data are not available are noted as N/A. (A) Average nucleotide identity percent similarity matrix; values ≥95% indicate that genomes belong to the same species. *Corynebacterium bovis* strains isolated from rodents (for example, mouse and rat) formed a distinct phylogenetic clade, which included *Corynebacterium* 1810230001 SH1 (inoculum strain) and *C. bovis* 2305220054 (output strain). *Corynebacterium* 1810230001 SH1 and *C. bovis* 2305220054 share >99.99% similarity, indicating they are likely identical strains. (B) Whole-genome phylogenetic tree built from core genes. *Corynebacterium bovis* strains isolated from rodents (for example, mouse, and rat) formed a distinct phylogenetic clade, which includes *Corynebacterium* 1810230001 SH1 and *C. bovis* 2305220054 (highlighted in yellow). *Corynebacterium* 1810230001 SH1 and *C. bovis* 2305220054 are most phylogenetically similar with each other since they are closely located on the same branch in the rodent clade.

Downloaded from https://prime-pdf-watermark.prime-prod.pubfactory.com/ at 2025-08-31 via free access

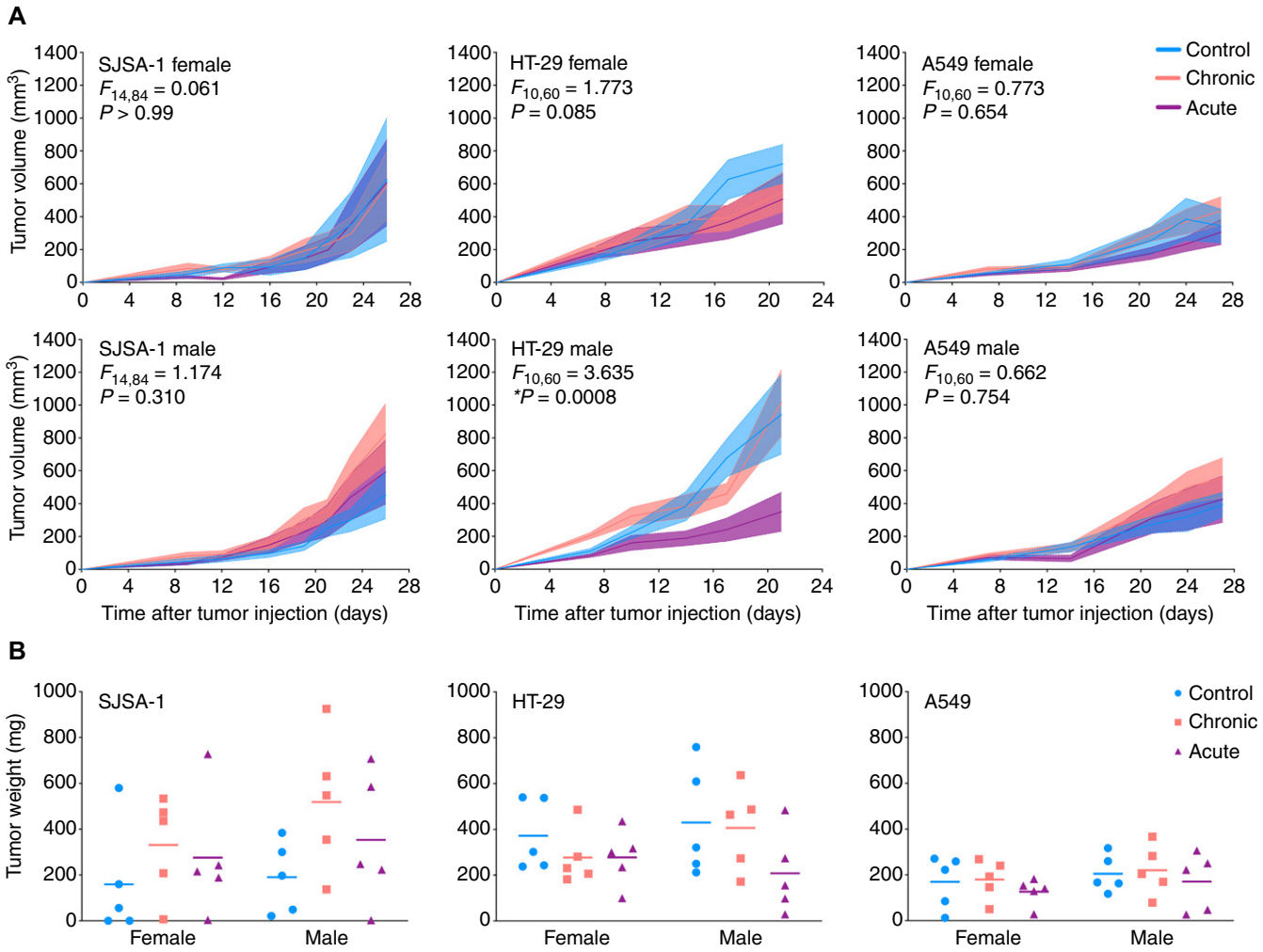

Figure 3. Tumor growth parameters of 3 different commonly used established human cancer cell lines (SJSA-1, HT-29, and A549) subcutaneously engrafted into the flanks of male and female nude mice in 1 of 3 experimental groups: 1) acutely infected with *Corynebacterium bovis* on the day of injection ('acute'; purple); 2) chronically infected with *C. bovis* 2 to 3 wk prior to injection ('chronic'; pink); 3) uninfected controls (blue). (A) Tumor growth rates plotted as mean volume ± SEM from day of injection until tumor collection (n = 5 per group). Rates only differed in the HT-29–injected males (two-way ANOVA, treatment × time; *, P = 0.0008); the acutely infected mice had significantly less growth by day 21 postinjection than both the control and chronically infected mice (Tukey's honestly significant difference test, P < 0.0001). (B) Final tumor weights as a scatter plot; horizontal lines represent the mean. No significant differences were found between groups.

between institutions, the goal of our study was to determine whether infection with *C. bovis* alters the growth characteristics of subcutaneous tumors under controlled study conditions using SPF mice. Although *S. xylosus* is not routinely excluded from most facilities, it is predicted that it may, on its own, cause clinical disease,[24] including hyperkeratosis. Mice used in our study were therefore confirmed to be negative for *S. xylosus* throughout the study to prevent potential confounding effects from coinfection. Growth of 3 human cell lines was monitored in male and female nude mice chronically or acutely infected with *C. bovis* and compared with uninfected CNT mice. There were no significant differences in the average tumor weights or final volumes for any of the cell lines between infection groups; however, these values trended smaller in females than in males. Importantly, HT-29–engrafted tumors grew significantly more slowly in AC males than in the CHR or CNT males, although no difference was present between the HT-29–engrafted female groups. In addition, for both males and females, the HT-29–engrafted AC groups had higher variability in volume and weight than did the CHR and CNT groups. These data suggest that infection with *C. bovis* alone did not prevent tumor engraftment for any of the cell lines assessed in this study. However, for some cell lines, the timing of *C. bovis* infection may differentially affect tumor growth characteristics, indicating that infection can negatively impact at least some tumor models.

Interestingly, none of the mice in our study exhibited gross CAH, and histologic analysis showed no hyperkeratosis, epidermal increased hyperplasia, or inflammation in either the AC or CHR groups compared with the CNT mice. Because *C. bovis* was first characterized as the cause of CAH in the 1990s,[2,3,13,25,26] investigations into its epidemiology have provided information on how the bacterium can spread as an aerosol or through contaminated fomites or biologics,[7,8] but the pathologic mechanisms behind the development of CAH have not been fully elucidated. Experimental infections with a pure *C. bovis* isolate do not consistently result in clinical dermatitis,[16] leading some groups to adopt a soiled-bedding transfer.[1,27] For example, Dole and colleagues applied pure cultures of 3 different isolates of *C. bovis* to naive nude mice; one isolate was associated with CAH, the second isolate was a mouse strain not associated with CAH, and the third isolate was from a cow. Regardless of the source, no differences were found in the growth or transmission of the isolates, and none caused significant hyperkeratosis or acanthosis.[16] However, in another study, when soiled bedding

Downloaded from Comparative Medicine Section via free access

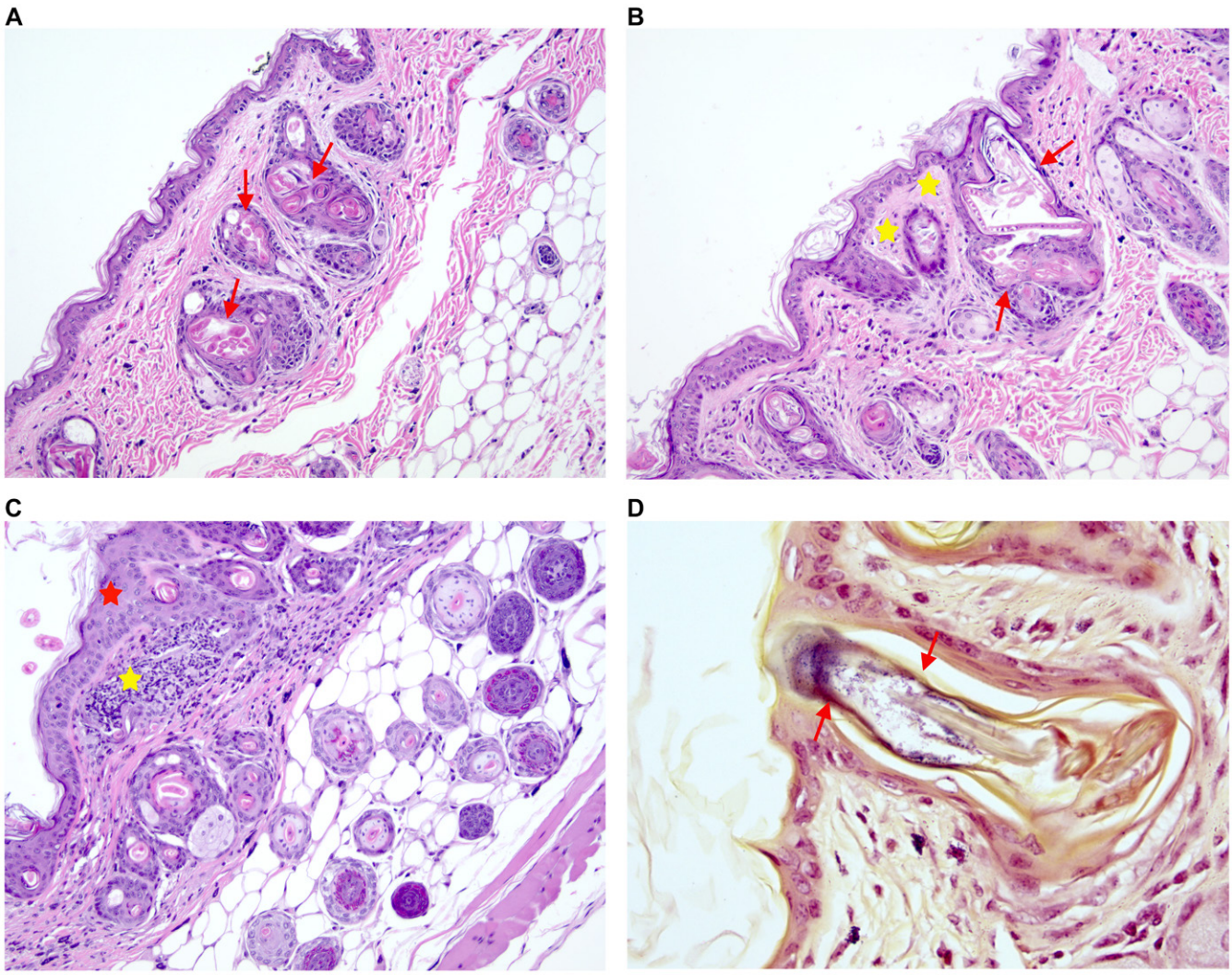

Figure 4. Examples of expected background findings in nude (*Foxn1*^{nu}) mice; representative images are shown but findings were similar across all tumor cohorts and between both sexes. Histologic hyperplasia and inflammation scores were not significantly elevated in the acute and chronic infection groups, compared with the controls, and appeared similar to these representative images. *Corynebacterium bovis* was not conclusively identified in sections from the experimentally infected groups, although infection was confirmed via molecular testing and dermal aerobic culture and isolation. (A) Twisting/coiling/fracture of the hair shafts and follicular keratosis (red arrows) in a SJSA-1–engrafted control male. Hematoxylin and eosin stain; original magnification, ×10. (B) Twisting/coiling/fracture of the hair shafts and follicular keratosis (red arrows) along with dermal fibrosis (yellow asterisks) in a HT-29–engrafted control male. Hematoxylin and eosin stain; original magnification, ×10. (C) Epidermal and infundibular hyperplasia (red asterisk) and folliculitis (yellow asterisk) in a A549-engrafted control female. Hematoxylin and eosin stain; original magnification, ×10. (D) Mixed Gram-positive and Gram-negative bacteria within the infundibulum (red arrows) in a A549-engrafted control female (different from female in C). Gram stain; original magnification, ×40.

was transferred from clinically ill mice, the onset of clinical disease was more consistent, with a high morbidity, and the incubation time was predictable.[27] The increased consistency of experimental induction of CAH using the soiled bedding suggests that either passage of the bacterium in vitro attenuates its virulence, or *C. bovis* alone is not sufficient for the development of disease.[27] If the latter case were true, clinical disease may be due to coinfection or exposure to other factors that, combined, cause inflammation.

The *C. bovis* isolate used in this study was collected from a mouse that presented with severe CAH at MIT in 2018. Whole-genome sequencing confirmed that this isolate was related to previously described rodent-specific CAH-associated isolates. *Staphylococcus xylosus* was also cultured from the affected mouse, demonstrating a coinfection that has been a common occurrence within MIT's facilities. Sequencing data from *C. bovis* isolated from the skin of infected mice at the end of study demonstrated >99% homology with the starting isolate, suggesting little genomic drift. However, unlike the mice used for the original isolate, the mice used in our current study remained free of *S. xylosus* throughout the study. The lack of hyperkeratosis and acanthosis in our infected mice suggests that these clinical signs typically attributed to *C. bovis* may actually result from coinfections with *C. bovis* and another organism such as *S. xylosus*.

Although CAH was not observed, mild acanthosis and hyperplasia were present in both infected and CNT mice histologically. This change has been seen previously and was thought to be secondary to one of the other microbes found on the skin of nude mice.[1] As we excluded *S. xylosus* in our study, it is possible that the low-grade acanthosis was due to another microbe such as an *Enterococcus* sp., which was isolated at high levels both at the beginning and end of our study. We interpreted the presence of Gram-positive rods within the infundibulum of the hair follicles of both the infected and CNT mice to be due to this or a similar commensal. However, the folliculitis noted

Downloaded from https://prime-pdf-watermark.prime-prod.pubfactory.com/ at 2025-08-31 via free access

Table 1. Summary of histologic analyses of experimentally naive male and female athymic nude mice

Tumor cohort	Sex	Infection group	Number analyzed	Mean epidermal hyperplasia and acanthosis score	Kruskal–Wallis *P* value	Mean dermal inflammation score	Kruskal–Wallis *P* value
SJSA-1	Male	Control	5	1.2	0.188	1.4	>0.99
		Chronic	3	1.7		1.3	
		Acute	3	2.0		1.7	
	Female	Control	5	1.8	0.883	1.8	0.491
		Chronic	3	2.3		2.3	
		Acute	3	2.0		1.7	
HT-29	Male	Control	5	1.8	>0.99	1.8	0.864
		Chronic	3	2.0		1.3	
		Acute	3	2.0		1.7	
	Female	Control	5	1.6	0.142	1.6	0.358
		Chronic	3	1.7		1.7	
		Acute	3	2.7		2.3	
A549	Male	Control	5	1.6	0.675	1.8	0.318
		Chronic	3	2.0		1.7	
		Acute	3	1.3		1.0	
	Female	Control	5	1.8	0.574	1.6	0.252
		Chronic	3	2.3		2.3	
		Acute	3	1.7		2.3	

Histology categories were graded on a scale of 1 to 3.[1]

in skin sections, regardless of infection status, has previously been noted as a background finding in nude mice.[14] Finally, the presence of nonexcluded commensals can also explain why *C. bovis* was identified easily through qPCR but not isolated by dermal swab in the infected HT-29 cohorts, as *C. bovis* grows slowly and others have found that overgrowth will make isolation more difficult.[2]

Our study focused on tumor type and time of infection only. However, the *C. bovis* isolate, strain of mouse, and/or the extent of immune compromise may also play a role in determining whether *C. bovis* alters tumor growth. For example, using naturally infected cohorts of mice displaying signs of clinical disease and uninfected CNT mice, Santos and colleagues engrafted 2 human carcinoma cell lines, MDA-MB-231 (mammary cancer) and SKVO3 (ovarian cancer), and monitored tumor growth over 60 d.[11] Nude mice with clinical disease displayed significant growth inhibition but NSG mice did not. This observed difference may be explained by the retained immune components in nude mice (for example, B cells, NK cells) that target engrafted tumor cells following an infectious or inflammatory insult.[2] It has previously been demonstrated that nude mice housed under barrier conditions have reduced NK cell cytotoxic activity compared with those housed under conventional conditions, likely due to increased exposure to opportunistic microbes.[28] In addition, the tumor microenvironment is thought to regulate the phenotype and function of NK cells to target primary and metastatic tumors, which can be harnessed therapeutically.[29–31] Thus, the underlying mechanism for engraftment failure in nude mice may in part be due to presence of functional NK cells. In addition, it is noteworthy that *S. xylosus* was not selectively excluded in that study.

Ideally, *C. bovis* is excluded from animal facilities that house mice used for cancer research. However, this is often not practical because the infection is widespread in many facilities, and tumor cell lines and patient-derived xenografts are commonly shared between facilities. Once a facility houses infected animals, it is extremely expensive and labor-intensive to eradicate the organisma, and reinfection is common. Therefore, practical alternative approaches are needed. One approach is prophylactic treatment with antibiotics. Treatment of infected nude and NSG mice with long-term amoxicillin has been shown to control clinical signs, although the infection is not cleared.[15] This may be a practical route for individuals working with patient-derived xenografts where preliminary testing of a portion of the tumor explant may lead to a false-negative result. However, although antibiotic-medicated feed had been used for years to manage CAH clinical disease, *Clostridioides difficile* overgrowth resulting in typhlocolitis in NSG mice has been reported following the therapeutic use of amoxicillin, resulting in peracute death, severe diarrhea with or without death, or mild diarrhea and recovery.[32] This event highlights one of the risks of broad-spectrum antibiotic use, in addition to antibiotic resistance and alteration of the microbiome,[15] which can affect tumor growth and alter the efficacy of cancer therapeutics.[33–37] Another approach used anecdotally by some laboratories is to intentionally expose incoming mice to infected animals and/or bedding in endemically infected facilities. This ensures that all animals are of the same health status at the time of tumor inoculation rather than risk mouse cages becoming infected at different times during the study, removing at least this one variable.

In summary, our results indicate that subclinical *C. bovis* infection in the absence of other inflammatory or infectious factors has little effect on skin pathology but may affect tumor growth characteristics depending on the tumor type. A limitation of this study is that only one strain of *C. bovis* and only one immunodeficient mouse strain (Crl:NU-*Foxn1*^{nu}) were used. We suggest that investigators working in shared facilities where *C. bovis* infection is present should consider running pilot studies to better understand the influence *C. bovis* may have on the models being used. Additional well-controlled studies are needed to determine how coinfection with *S. xylosus* and potentially other inflammatory or infectious conditions effect tumor engraftment and growth.

Downloaded from Comparative Medicine Section via free access

Supplementary Materials

Table S1. *Corynebacterium bovis* strains included in genome sequencing analysis[16,38–40]

Acknowledgments

We thank Erin Mathieu, Sam Ros, Brian Lagace, Suzette J. Morales, Ellen Jordan, and Caroline Atkinson and Ed Clark from the MIT DCM Histology Laboratory for technical support. We also thank Dr. Gerardo Mendoza for the helpful discussion and suggestions.

Conflict of Interest

The authors have no conflicts of interest to declare.

Funding

This work was generously supported by a 2022 American College of Laboratory Animal Medicine Foundation Grant (to H.R.H. and A.A.B.). Portions of this research were conducted within the Koch Institute's Preclinical Modeling facility or the MIT BioMicro Center, which are supported by Core Grant P30-CA14051 from the National Cancer Institute.

Author Contributions

A.G.B., H.R.H., A.A.B., T.M.A., K.S.H., and G.B.M. designed the research study; A.A.B. performed all aspects of the tumor cell culture and injection; A.G.B., H.R.H., and A.A.B. cared for the animals in the study and performed all in vivo work; A.G.B. performed all inoculations and molecular assays; A.M. performed all whole-genome sequencing analyses; M.B. performed the histologic analyses; and A.G.B., H.R.H., and A.A.B. wrote the first draft of the paper. All authors reviewed and critically edited the manuscript.

References

1. Burr HN, Lipman NS, White JR, Zheng J, Wolf FR. Strategies to prevent, treat, and provoke *Corynebacterium*-associated hyperkeratosis in athymic nude mice. *J Am Assoc Lab Anim Sci.* 2011;50(3):378–388.
2. Scanziani E, Gobbi A, Crippa L, et al. Outbreaks of hyperkeratotic dermatitis of athymic nude mice in Northern Italy. *Lab Anim.* 1997;31(3):206–211.
3. Scanziani E, Gobbi A, Crippa L, et al. Hyperkeratosis-associated coryneform infection in severe combined immunodeficient mice. *Lab Anim.* 1998;32(3):330–336.
4. Vedder AR, Miedel EL, Ragland NH, et al. Effects of *Corynebacterium bovis* on engraftment of patient-derived chronic-myelomonocytic leukemia cells in NSGS mice. *Comp Med.* 2019;69(4):276–282.
5. Gozalo AS, Hoffmann VJ, Brinster LR, Elkins WR, Ding L, Holland SM. Spontaneous *Staphylococcus xylosus* infection in mice deficient in NADPH oxidase and comparison with other laboratory mouse strains. *J Am Assoc Lab Anim Sci.* 2010;49(4):480–486.
6. Russo M, Invernizzi A, Gobbi A, Radaelli E. Diffuse scaling dermatitis in an athymic nude mouse. *Vet Pathol.* 2013;50(4):722–726.
7. Burr HN, Wolf FR, Lipman NS. *Corynebacterium bovis*: epizootiologic features and environmental contamination in an enzootically infected rodent room. *J Am Assoc Lab Anim Sci.* 2012;51(2):189–198.
8. Manuel CA, Pugazhenthi U, Spiegel SP, Leszczynski JK. Detection and elimination of *Corynebacterium bovis* from barrier rooms by using an environmental sampling surveillance program. *J Am Assoc Lab Anim Sci.* 2017;56(2):202–209.
9. Vedder A, Miedel EL, Ragland NH, et al. Primary patient-derived xenografts in NSG-S mice show variable engraftment when infected with *Corynebacterium bovis* [abstract PS127]. *J Am Assoc Lab Anim Sci.* 2017;56(5):691–692.
10. Pearson EC, Pugazhenthi U, Fong DL, et al. Metaphylactic antibiotic treatment to prevent the transmission of *Corynebacterium bovis* to immunocompromised mouse offspring. *J Am Assoc Lab Anim Sci.* 2020;59(6):712–718.
11. Santos M, Chandler A, Valdivia A, et al. *Corynebacterium bovis* infection of immunocompromised mice variably impacts tumor xenografts [abstract P207]. *J Am Assoc Lab Anim Sci.* 2016;55(5):660.
12. Vedder A, Miedel E, Ragland N, et al. The opportunistic pathogen *Corynebacterium bovis* augments leukemia patient derived xenograft engraftment: a cautionary tale [abstract RES-190]. *Clin Lymphoma Myeloma Leuk.* 2017;17:S392.
13. Field K, Greenstein G, Smith M, Herrmann S, Gizzi J. Hyperkeratosis-associated coryneform in athymic nude mice. *Lab Anim Sci.* 1995;(45):469.
14. Mendoza G, Cheleuitte-Nieves C, Lertpiriyapong K, et al. Establishing the median infectious dose and characterizing the clinical manifestations of mouse, rat, cow, and human *Corynebacterium bovis* isolates in select immunocompromised mouse strains. *Comp Med.* 2023;73(3):200–215.
15. Manuel CA, Johnson LK, Pugazhenthi U, et al. Effect of antimicrobial prophylaxis on *Corynebacterium bovis* infection and the skin microbiome of immunodeficient mice. *Comp Med.* 2022;72(2):78–89.
16. Dole VS, Henderson KS, Fister RD, Pietrowski MT, Maldonado G, Clifford CB. Pathogenicity and genetic variation of 3 strains of *Corynebacterium bovis* in immunodeficient mice. *J Am Assoc Lab Anim Sci.* 2013;52(4):458–466.
17. Olson RD, Assaf R, Brettin T, et al. Introducing the bacterial and viral bioinformatics resource center (BV-BRC): a resource combining PATRIC, IRD and ViPR. *Nucleic Acids Res.* 2023;51(D1):D678–D689.
18. Pritchard L, Glover RH, Humphris S, Elphinstone JG, Toth IK. Genomics and taxonomy in diagnostics for food security: soft-rotting enterobacterial plant pathogens. *Anal Methods.* 2016;8(1):12–24.
19. Emms DM, Kelly S. OrthoFinder: phylogenetic orthology inference for comparative genomics. *Genome Biol.* 2019;20(1):238.
20. Hoffman-Luca CG, Yang CY, Lu J, et al. Significant differences in the development of acquired resistance to the MDM2 inhibitor SAR405838 between in vitro and in vivo drug treatment. *PLoS One.* 2015;10(6):e0128807.
21. Warin R, Xiao D, Arlotti JA, Bommareddy A, Singh SV. Inhibition of human breast cancer xenograft growth by cruciferous vegetable constituent benzyl isothiocyanate. *Mol Carcinog.* 2010;49(5):500–507.
22. National Centre for the Replacement, Refinement & Reduction of Animals in Research. Group and sample size. Updated November 30, 2023. Accessed October 12, 2021. https://eda.nc3rs.org.uk/experimental-design-group.
23. Mecklenburg L, Tychsen B, Paus R. Learning from nudity: lessons from the nude phenotype. *Exp Dermatol.* 2005;14(11):797–810.
24. Reshamwala K, Cheung GYC, Hsieh RC, et al. Identification and characterization of the pathogenic potential of phenol-soluble modulin toxins in the mouse commensal *Staphylococcus xylosus*. *Front Immunol.* 2022;13:999201.
25. Clifford CB, Walton BJ, Reed TH, Coyle MB, White WJ, Amyx HL. Hyperkeratosis in athymic nude mice caused by a coryneform bacterium: microbiology, transmission, clinical signs, and pathology. *Lab Anim Sci.* 1995;45(2):131–139.
26. Duga S, Gobbi A, Asselta R, et al. Analysis of the 16S rRNA gene sequence of the coryneform bacterium associated with hyperkeratotic dermatitis of athymic nude mice and development of a PCR-based detection assay. *Mol Cell Probes.* 1998;12(4):191–199.
27. Manuel CA, Pearson EC, Pugazhenthi U, et al. A clinical scoring systems for the evaluation of *Corynebacterium bovis*-associated disease in NSG mice. *Comp Med.* 2022;72(6):386–393.
28. Hanna N, Davis TW, Fidler IJ. Environmental and genetic factors determine the level of NK activity of nude mice and affect their suitability as models for experimental metastasis. *Int J Cancer.* 1982;30(3):371–376.
29. López-Soto A, Gonzalez S, Smyth MJ, Galluzzi L. Control of metastasis by NK cells. *Cancer Cell.* 2017;32(2):135–154.
30. Morvan MG, Lanier LL. NK cells and cancer: you can teach innate cells new tricks. *Nat Rev Cancer.* 2016;16(1):7–19.

Downloaded from https://prime-pdf-watermark.prime-prod.pubfactory.com/ at 2025-08-31 via free access

31. Paul S, Lal G. The molecular mechanism of natural killer cells function and its importance in cancer immunotherapy. *Front Immunol.* 2017;8:1124.
32. Ma KGL, Lertpiriyapong K, Piersigilli A, et al. Outbreaks of typhlocolitis caused by hypervirulent group ST1 *Clostridioides difficile* in highly immunocompromised strains of mice. *Comp Med.* 2020;70(3):277–290.
33. Cheung MK, Yue GGL, Tsui KY, et al. Discovery of an interplay between the gut microbiota and esophageal squamous cell carcinoma in mice. *Am J Cancer Res.* 2020;10(8):2409–2427.
34. Gopalakrishnan V, Spencer CN, Nezi L, et al. Gut microbiome modulates response to anti–PD-1 immunotherapy in melanoma patients. *Science.* 2018;359(6371):97–103.
35. Matson V, Fessler J, Bao R, et al. The commensal microbiome is associated with anti–PD-1 efficacy in metastatic melanoma patients. *Science.* 2018;359(6371):104–108.
36. Sethi V, Kurtom S, Tarique M, et al. Gut microbiota promotes tumor growth in mice by modulating immune response. *Gastroenterology.* 2018;155(1):33–37.e6.
37. Thomas RM, Gharaibeh RZ, Gauthier J, et al. Intestinal microbiota enhances pancreatic carcinogenesis in preclinical models. *Carcinogenesis.* 2018;39(8):1068–1078.
38. Cheleuitte-Nieves C, Gulvik CA, McQuiston JR, et al. Genotypic differences between strains of the opportunistic pathogen *Corynebacterium bovis* isolated from humans, cows, and rodents. *PLoS One.* 2018;13(12):e0209231.
39. Tatusova T, Ciufo S, Fedorov B, O'Neill K, Tolstoy I. RefSeq microbial genomes database: new representation and annotation strategy. *Nucleic Acids Res.* 2014;42(Database issue):D553–D559.
40. Sichtig H, Minogue T, Yan Y, et al. FDA-ARGOS is a database with public quality-controlled reference genomes for diagnostic use and regulatory science. *Nat Commun.* 2019;10(1):3313.

Downloaded from https://prime-pdf-watermark.prime-prod.pubfactory.com/ at 2025-08-31 via free access